Experimental and theoretical investigation of Gabapentin by Density functional theory

P.S.Ganeshvar[#], M.Kanagaraj[#,*], S.Gunasekaran[¥], T.Gnanasambandan[¶]

Abstract— The FT-IR and FT-Raman spectra of Gabapentin (GBT) have been recorded in the region 4000–400 and 3500–100 cm-1 respectively. The optimized geometry, frequency and intensity of the vibrational bands were obtained by the density functional theory (DFT) using 6-31G(d,p) basis set. The harmonic vibrational frequencies were scaled and compared with experimental values. The observed and the calculated frequencies were found to be in good agreement. The UV–visible spectrum was also recorded and compared with the theoretical values. The calculated HOMO and LUMO energies show that charge transfer occurs within the molecule. The Mulliken charges of the molecule were also computed using DFT calculations. Stability of the molecule arising from hyper conjugative interactions, charge delocalization were analyzed using natural bond orbital (NBO) analysis. Information about the charge density distribution of the molecule and its chemical reactivity were obtained by mapping molecular electrostatic potential surface. In addition, the non-linear optical properties were discussed from the dipole moment values and the excitation wavelength in the UV–visible region.

Index Terms— FT-IR, FT-Raman, DFT, GBT, NBO.

1 INTRODUCTION

Gabapentin, chemically known as 2-[1-(AminoMethyl) Cyclohexyl]Acetic acid, works by stabilizing electrical activity in the brain. Gabapentin interacts with cortical neurons at auxiliary subunits of voltage-sensitive calcium channels and increases the synaptic concentration of GABA (Gamma- Aminobutyric acid), enhances GABA responses at non-synaptic sites in neuronal tissues, and reduces the release of mono-amine neurotransmitters.

Gabapentin and its derivatives had been studied by several authors. Advances in simultaneous DSC–FTIR microspectroscopy for rapid solid-state chemical stability studies: Some dipeptide drugs as examples were carried out by Shan-Yang Lin et al. [1]. Gabapentin adjunctive therapy in neuropathic pain sites were investigated by H.Rosner et al. [2]. The use of Gabapentin as a new agent for the management of epilepsy was studied by C.O.Andrews et.al[3]. Functionalization of carboxylated multiwall nanotubes with Gabapentin and Baclofen, and also study of their antibacterial activities against E.coli and S. aureus were reported by Javad Azizian et al. [4]. Novel Challenges in Crystal Engineering: Polymorphs and New Crystal Forms of Active Pharmaceutical Ingredients were carried out by Vânia André et al. [5].

In the present work, harmonic-vibrational frequencies are calculated for Gabapentin (GBT) using B3LYP with 6-31G(d,p) method. The calculated spectra of the compound are compared to that of experimentally observed FT-IR and FT-Raman spectra. The redistribution of electron density (ED) in various bonding and antibonding orbitals and E(2) energies were calculated by natural bond orbital (NBO) analysis by DFT method to give clear evidence of stabilization originating from the hyper conjugation of various intramolecular interactions. The HOMO and LUMO analysis were used to elucidate information regarding ionization potential (IP), electron affinity (EA), electronegativity (χ), electrophilicity index (ω), hardness (η) and chemical potential (μ) which are all correlated. All these confirm the charge transfer within the molecule and also molecular electrostatic potential (MESP) contour map also shows various electrophilic regions of the title molecule.

- *P.S.Ganeshvar is currently pursuing doctoral degree program in department of physics, Karpagam University, Coimbatore-641021. Tamilnadu, India.*
- *Corresponding author: Dr. M. Kanagaraj is currently Assistant professor in department of physics, Karpagam University, Coimbatore-641021. Tamilnadu, India.E-mail: kanaguphy@gmail.com.*
- *Dr. S. Gunasekaran is currently Professor in Research & Development St.Peter's Institute of Higher Education and Research, St.Peter's University, Avadi, Chennai -600 054. Tamilnadu, India.*
- *T.Gnanasambandan is currently Professor in Department of Physics, Pallavan College of Engineering, Kanchipuram -631 502. Tamilnadu, India*

2 MATERIALS AND METHODS

2.1 Spectroscopic measurements

For the study, the compound Gabapentin (GBT) in the solid form was purchased from Sigma–Aldrich Chemical Company (USA) with a stated purity of 98% and it was used as such without further purification. The FT-Raman spectrum of GBT was recorded using 1064 nm line of Nd: YAG laser as excitation wavelength in the region 3500–100 cm–1 on a Thermo Electron Corporation model Nexus 670 spectrometer equipped with FT-Raman module accessory. The FT-IR spectrum of this compound was recorded in the range of 4000–400 cm–1on Nexus 670 spectrophotometer using KBr pellet technique at room temperature with a spectral resolution of 4.0 cm–1. The ultraviolet absorption spectrum of GBT solved in water was examined in the range 200–400 nm by using Cary 5E UV–Visible NIR recording spectrometer.

2.2 Computational details

Quantum chemical calculations were used to carry out the optimization of the geometry and to determine the vibrational wavenumbers of Gabapentin (GBT), with the 2003 version of the Gaussian suite [6] using the DFT(B3LYP) method [7,8] supplemented with standard 6-31G(d,p) basis set. The vibrational modes were assigned by means of visual inspection us-

ing GAUSSVIEW program [9]. The vibrational mode analysis of GBT was presented in some detail in order to better describe the basis for the assignments, from the basic theory of Raman scattering. A comparison was made between the theoretically calculated frequencies and the experimentally measured frequencies. In this investigation the researchers observed that the calculated frequencies were slightly greater than the fundamental frequencies. To improve the agreement between the predicted and observed frequencies, the computed harmonic frequencies are usually scaled for comparison. The vibrational modes were assigned on the basis of PED analysis using VEDA 4 program [10].

3 Results and Discussion

3.1 Molecular geometry

The energetically most stable optimized geometry obtained by B3LYP/6-31G(d,p) method and the scheme of numbering the atoms of the molecules Gabapentin (GBT) are shown in Fig. 1. The global minimum energy obtained for GBT are calculated as -558.431521 Hartrees, by B3LYP functional with the standard 6-31G(d,p) basis set respectively. The calculated optimized geometrical parameters such as bond length and bond angle are presented in Table 1 respectively.

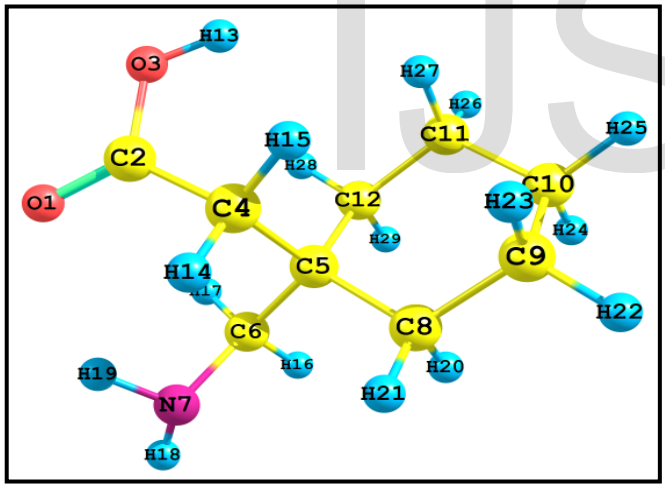

Fig. 1. Optimized structure of GBT

3.2 Vibrational assignments

From the structural point of view, the title compound was assumed to have C1 point group symmetry and hence all the calculated frequency transforming to the same symmetry species (A). The molecule GBT consists of 29 atoms and 81 internal modes of vibrations. Molecular symmetry describes the symmetry present in the molecule, which can predict or explain many of a molecule's chemical properties, such as its dipole moment and its allowed spectroscopic transitions. The observed and calculated frequencies of GBT, compared and characterized by PED, are summarized in Table 2 respectively. All the vibrations are active in both IR and Raman. For visual comparison, the observed and simulated FT-IR and FT-Raman spectra of GBT are shown in Figs. 2-3.

TABLE 1
OPTIMIZED GEOMETRICAL PARAMETERS OF GBT

Bond length(Å)	B3LYP 6-31G(d,p)	Bond angle(°)	B3LYP 6-31G(d,p)	Bond angle(°)	B3LYP 6-31G(d,p)
O1-C2	1.210	O1-C2-O3	119.18	C5-C6-H16	107.46
C2-O3	1.361	O1-C2-C4	123.99	C5-C6-H17	108.66
C2-C4	1.519	O3-C2-C4	116.81	N7-C6-H16	108.58
O3-H13	0.968	C2-O3-H13	109.88	N7-C6-H17	112.97
C4-C5	1.563	C2-C4-C5	113.83	H16-C6-H17	106.46
C4-H14	1.092	C2-C4-H14	106.80	C6-N7-H18	109.69
C4-H15	1.094	C2-C4-H15	110.27	C6-N7-H19	108.39
C5-C6	1.550	C5-C4-H14	107.76	H18-N7-H19	106.56
C5-C8	1.550	C5-C2-H15	110.34	C5-C8-C9	114.07
C5-C12	1.549	H14-C4-H15	107.55	C5-C8-H20	107.48
C6-N7	1.467	C4-C5-C6	109.19	C5-C8-H21	109.14
C6-H16	1.096	C4-C5-C8	108.64	C9-C8-H20	108.12
C6-H17	1.102	C4-C5-C12	111.86	C9-C8-H21	111.45
N7-H18	1.016	C6-C5-C8	109.65	H20-C8-H21	106.19
N7-H19	1.019	C6-C5-C12	108.39	C8-C9-C10	111.33
C8-C9	1.537	C8-C5-C12	109.08	C8-C9-H22	107.41
C8-H20	1.099	C5-C6-N7	112.39	C8-C9-H23	110.53
C8-H21	1.094	C10-C9-H22	110.11	C10-C11-C12	117.74
C9-H10	1.536	C10-C9-H23	109.52	C10-C11-H26	110.38
C9-H22	1.096	H22-C9-H23	105.79	C10-C11-H27	108.82
C9-H23	1.099	C9-C10-C11	111.40	C12-C11-H26	109.52
C10-C11	1.536	C9-C10-H24	108.99	C12-C11-H27	110.52
C10-H24	1.099	C9-C10-H25	110.35	H26-C11-H27	105.67
C10-H25	1.096	H24-C10-H25	106.52	C5-C12-C11	114.16
C11-C12	1.538	C5-C12-H28	110.23	C11-C12-H29	108.19
C11-H26	1.096	C5-C12-H27	107.74	H28-C12-H29	105.81
C11-H27	1.010	C11-C12-H28	110.31		
C12-H28	1.097				
C12-H29	1.099				

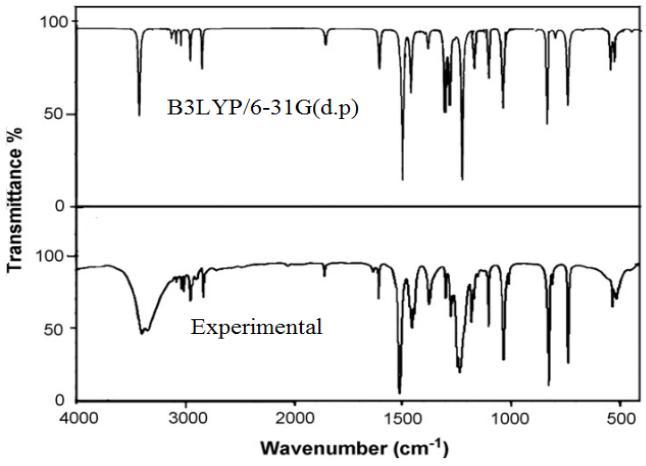

Fig. 2. FT-IR spectra of GBT

3.2.1 C–C vibrations

The bands between 1400 and 1650 cm−1 in the aromatic and hetero aromatic compounds are assigned to carbon vibrations [11]. The actual positions are determined not by the nature of the substituents but rather by the form of the substitution around the aromatic ring. Moreover, when C–N or more double modes are in conjugation, the delocalization of π-

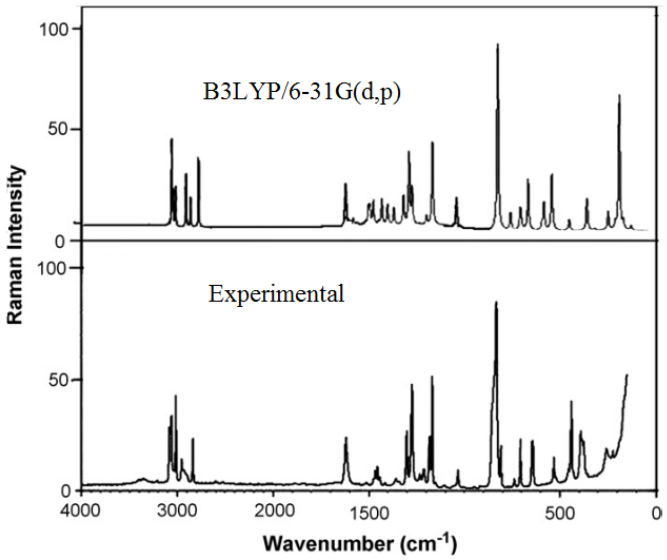

Fig. 3. FT-Raman spectra of GBT

electrons result in a transfer of some bond order to intervening single bonds and hence, there is full in the carbon–carbon stretching frequency. In this study the FT-IR bands observed at 1524, 1499 and 1400 cm−1 and Raman bands observed at 1523, 1499 and 1400 cm−1 have been assigned to carbon–carbon stretching vibration. In the calculated, value the stretching vibrations are observed at 1400 cm−1 in 6-31G(d,p) basis set.

TABLE 2
VIBRATIONAL ASSIGNMENTS OF GBT

Mode No	Experimental frequency		Calculated frequency	Vibrational Band Assignments (PED %)
	FT-IR (vcm^{-1})	FT-R(vcm^{-1})		
1.	3491	3491	3491	νNH(100)
2.	3130	3130	3130	νCH(99)
3.	3097	3097	3097	νCH(59)
4.	3076	3076	3077	νCH(47)
5.	3070	3070	3071	νCH(61)
6.	3061	3061	3060	νCH(50)
7.	3029	3028	3029	νCH(95)
8.	3024	3024	3025	νCH(88)
9.	3022	3022	3021	νCH(91)
10.	3018	3018	3018	νCH(99)
11.	2994	2995	2994	νCH(93)
12.	2980	2980	2980	νCH(94)
13.	1850	1850	1850	νOC(84)
14.	1676	1676	1676	δHNH(70)+τHNCC(13)
15.	1524	1523	1524	νCC(76)
16.	1518	1518	1518	δHCH(14)+υCC(51)+βCCC(10)
17.	1512	1512	1512	δHCH(17)+υCC(39)
18.	1506	1506	1506	δHCH(19)+υCC(48)
19.	1499	1499	1500	δHCH(15)+υCC(14)+βHCC(32)
20.	1499	1499	1499	δHCH(58)
21.	1494	1493	1494	δHCH(38)+τHCCC(11)+βHCH(18)
22.	1427	1427	1427	δHCH(14)+βHCO(50)
23.	1400	1400	1400	τHCCC(14)+υCC(10)+βHCO(41)
24.	1396	1396	1396	δHCCC(10)
25.	1389	1389	1389	τHCCC(21)+υCC(55)
26.	1377	1377	1377	δHCN(13)+υCC(51)+βCCC(10)
27.	1375	1375	1375	τHCCC(10)
28.	1357	1358	1357	τHCCC(11)
29.	1339	1339	1339	τHCCO(14)
30.	1329	1329	1329	τHCCC(10)
31.	1311	1310	1311	δHCC(16)+τHCCC(15)
32.	1299	1298	1299	δHCC(14)+τHCCC(10)
33.	1293	1294	1293	δHCC(16)+τHCCC(10)
34.	1264	1265	1264	δHCC(23)
35.	1231	1231	1231	δHCN(13)
36.	1221	1221	1221	δHCN(26)
37.	1191	1192	1191	νCC(13)
38.	1166	1165	1166	δHCC(11)
39.	1138	1138	1138	δHNC(11)+δHCN(12)
40.	1117	1117	1117	δHCC(10)
41.	1099	1099	1099	νNC(35)
42.	1089	1088	1089	νCC(16)
43.	1064	1065	1064	δHCC(11)
44.	1042	1042	1042	νCC(18)
45.	999	999	999	δHNC(14)
46.	985	984	985	νCC(10)
47.	966	966	966	δCCC(12)
48.	948	947	948	τHCCC(10)
49.	914	914	914	τHNCC(11)
50.	892	891	892	νOC(20)+νCC(29)
51.	886	885	886	νCC(19)
52.	862	862	862	τHCCC(10)
53.	859	858	859	τHCCC(20)
54.	831	831	831	νCC(29)
55.	792	791	792	νCC(15)+τHCCC(14)
56.	786	785	786	δOCOC(20)
57.	679	679	679	νCC(20)+δOCO(26)
58.	605	604	605	δOCO(38)+δOCOC(19)
59.	580	579	580	δCCC(13)+δCCCC(71)
60.	516	515	516	τHOCC(74)
61.	502	502	502	δCCC(13)+τHOCC(10)
62.	469	469	469	δOCC(45)+τHCCO(12)
63.	459	459	459	δCCC(15)
64.	-	432	432	δCCCC(18)
65.	-	397	397	δCCC(12)
66.	-	351	352	τCCCC(11)+δCCCC(10)
67.	-	334	335	τHNCC(62)
68.	-	316	316	δCCC(12)
69.	-	278	278	δCCC(11)+δCCCC(13)
70.	-	230	231	τCCCC(18)
71.	-	216	215	δCCC(42)+δOCOC(10)
72.	-	156	155	δCCC(20)
73.	-	145	144	δCCC(33)
74.	-	137	136	δCCC(10)
75.	-	89	90	δCCC(11)
76.	-	54	55	τCCC(47)+τOCCC(46)

3.2.2 C–H vibration

The substituted benzene like molecule gives rise to C–H stretching, C–H in-plane and C–H out-of-plane bending vibration. Aromatic compounds commonly exhibit multiple weak bands in the region 3200–3000 cm−1 due to aromatic C–H stretching vibrations. The bands due to C–H in-plane bending vibrations interact somewhat with C–C stretching vibrations are observed as a number of bands in the region 1300–1000 cm−1. The C–H out-of-plane bending vibrations occur in the

region 900–667 cm−1 [12, 13]. In this region the bands are not affected appreciable by the nature of the substituents. In the present investigations, the FT-IR bands identified at 3130, 3097, 3018 cm−1and FT-Raman bands at 3130, 3097, 3018 cm−1 are assigned C–H stretching vibrations. The FT-IR and FT-Raman bands observed at 1311, 1264 and 1310, 1265 cm−1 were assigned to C–H in-plane bending vibrations.

3.2.3 C-N vibration

The identification of wavenumber for C–N stretching in the side chains is rather difficult since there are problems in differentiating that wavenumber from others. Arivazhagan et al. [14] assigned 1635 cm–1 for 5-nitro-2-furaldehyde oxime for C–N vibration. Sengamalai et al. [15] assigned the C–N stretching at 1325 cm–1 in 2-methyl-6-nitroquinoline. Arivazhagan et al. [16] assigned 2238 cm–1 for p-fluoro benzonitrile for C–N vibration. In the present investigation, the observed bands at 1676, 1377 and 1221 cm–1 in IR are assigned to C–N stretching vibration. The C=N stretching is assigned to the wavenumber 1676 cm–1 in FTIR spectrum. These values support the reported results [14,15].

3.2.4 Carboxylic and carbonyl vibrations

The carbonyl stretching frequency has been most extensively studied by infrared spectroscopy [17]. This multiply bonded group is highly polar and therefore gives rise to an intense infrared absorption band. The carbon–oxygen double bond is formed by pπ–pπ bonding between carbon and oxygen. Because of the different electro negativities of carbon and oxygen atoms, the bonding electrons are not equally distributed between the two atoms. The lone pair of electrons on oxygen also determines the nature of the carbonyl group. The carbonyl stretching vibrations are found in the region 1780–1700 cm-1 [18]. In GBT, the band appearing at 1850 cm-1 (FT-IR) belongs to C=O group. The corresponding calculated wavenumber is at 1850 cm-1 using B3LYP/ 6-31G(d,p) basis set. The bands related to C=O bending mode are weak and complicated [19]. It is a highly mixed mode as it is evident from Table 2. However, the band observed 892 cm-1 in both the FT-IR and FT-Raman spectra is assigned to C=O in-plane bending modes. The frequencies calculated at 786 and 605 cm-1 in B3LYP are assigned to C=O out-of-plane bending vibrations which are not observed in either of the spectra.

3.2.5 N–H vibrations

It has been observed that the presence of N–H group in various molecules may be correlated with a constant occurrence of absorption bands whose positions are slightly altered from one compound to another; this is because the atomic group vibrates independently of the other groups in the molecule and has its own frequency. The position of absorption in this region depends upon the degree of hydrogen bonding, and hence upon the physical state of the sample. Normally in all the heterocyclic compounds, the N–H stretching vibration occurs in the region of 3500–3000 cm−1 [20].

In the title molecule, the N–H stretching vibration is predicted at 3491 cm−1 by B3LYP/6-31G (d,p) and is in very good agreement with experimental methods. This mode is pure stretching mode as it is evident from Table 2, which is exactly contributing to 100% of PED. This predicted wavenumber is exactly correlated with the literature data [17].

3.3 Other molecular properties

3.3.1 Natural bond orbital analysis

Natural bond orbital (NBO) analysis provides an efficient method for studying intra- and intermolecular bonding and interaction among bonds and also provides a convenient basis for investigating charge transfer or conjugative interaction in molecular systems [21]. Higher magnitude of E(2) value indicates intensive interaction between electron donors and electron acceptors and hence greater will be the extent of conjugation. Delocalization of electron density between occupied Lewis-type (bond or lone pair) NBO orbitals and formally unoccupied [antibond or Rydgberg] non-Lewis NBO orbitals correspond to a stabilizing donor-acceptor interaction. NBO analysis has been performed on the title molecule GBT at the B3LYP/6-31G(d,p) level in order to elucidate the delocalization of electron density within the molecule. The intramolecular interactions are formed by the orbital overlap between bonding LP(2) O1, LP (2) O1, LP(2) O3, LP(1) O3, LP(1) N7, LP(1) N7 and antibonding σ*(C2-O3), σ*(C2-O4), π*(O1-C2), σ*(C2-C4), σ*(C5-C6), σ*(C6-H17) orbital which results in ICT causing stabilization of the system. The second-order perturbation theory of Fock matrix in the NBO analysis shows strong intramolecular hyperconjugative interactions and the results are presented in Table 3. The most important interaction observed are LP(2) O3→π*(O1-C2), LP(2)O1→σ*(C2-O3), LP(2)O1→σ*(C2-O3) and the corresponding energies were 44.58, 35.79 and 15.20 KJ/mol respectively. This larger energy provides the stabilization to the molecular structure. Graphical representation of intramolecular interaction is presented in Fig.4.

TABLE 3
SECOND ORDER PERTURBATION THEORY ANALYSIS OF FOCK MATRIX IN NBO ANALYSIS

Donor(i)	Acceptor(j)	E(2)[a] (kJ/mol)	E(j)–E(i)[b] (a.u.)	F(i, j)[c] (a.u.)
LP(2)O1	σ*(C2-O3)	35.79	0.53	0.124
LP(2)O1	σ*(C2-C4)	15.20	0.63	0.090
LP(1)O3	σ*(C2-C4)	4.80	0.95	0.061
LP(2)O3	π*(O1-C2)	44.58	0.31	0.106
LP(1)N7	σ*(C5-C6)	5.71	0.59	0.052
LP(1)N7	σ*(C6-H17)	5.79	0.69	0.57

a E(2) means energy of hyper conjugative interaction (stabilization energy).
b Energy difference between donor and acceptor i and j NBO orbitals.
c F(i,j) is the fock matrix element between i and j NBO orbitals.

3.3.2 Molecular electrostatic potential

Molecular electrostatic potential(MEP) at a point in the space around a molecule gives an indication of the net electrostatic effect produced at that point by the total charge distribution(electron+nuclei) of the molecule and correlates with dipolemoments, electronegativity, partial charges and chemical reactivity of the molecule. It provides a visual method to understand the relative polarity of the molecule. An electron-density isosurface mapped with electrostatic potential surface depicts the size, shape, charge density and site of chemical reactivity of the molecule. Such mapped electrostatic potential surface has been plotted for the title molecule in 6-31G(d,p) basis set using the computer software Gauss view 05[9] . A projection of this surface along the molecular plane is given in Fig.5. The different values of the electrostatic potential at the surface are represented by different colors: red represents regions of most negative electrostatic potential, blue represents regions of most positive electrostatic potential and green represents regions of zero potential. Potential increases in the order: red<orange<yellow<green<blue.

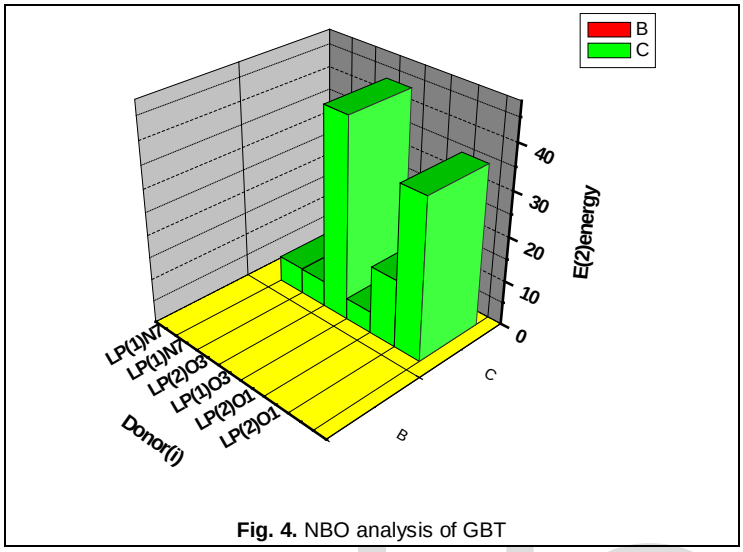

Fig. 4. NBO analysis of GBT

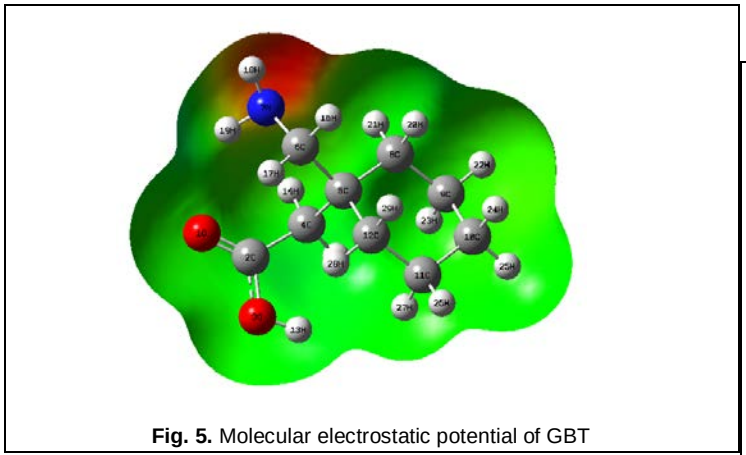

Fig. 5. Molecular electrostatic potential of GBT

In all cases, the shape of the electrostatic potential surface is influenced by the structure and charge density distributions in the molecule with sites close to the oxygen atom, showing regions of most negative electrostatic potential. The calculated 3D MEP shows the negative regions are electrophilic region, these are mainly due to N7, O1 and O3 atoms. The positive regions are the nucleophilic region and these are over the hydrogen atoms of the title molecule GBT. As mentioned earlier, the electrostatic potential has been used primarily for predicting sites and relative reactivities towards electrophilic attack and in studies of biological recognition and hydrogen bonding interactions [22, 23].

3.3.3 UV–Vis spectrum and HOMO-LUMO energy gap

Many organic molecules containing conjugated π electron, characterized by large values of molecular first-order hyperpolarizabilities, are analyzed by means of vibrational spectroscopy [24]. In most cases, even in the absence of inversion symmetry, the strongest band in the Raman spectrum is weak in the IR spectrum and vice versa. But the intramolecular charge from the donor to the acceptor group through a single-double bond conjugated path can induce large variations of both the molecular dipole moment and the molecular polarizability, making FT-IR and FT-Raman activity strong at the same time. The experimental spectroscopic behaviour described above is well accounted for DFT calculations in π conjugated systems that predict exceptionally infrared intensities for the same normal modes. The analysis of the wavefunction indicate that the electronic absorption corresponds to the transition from the ground to the first excited state and is mainly described by one electron excitation from the highest occupied molecular orbital (HOMO) to the lowest unoccupied molecule orbital (LUMO). The energy gap of the title molecule is calculated at B3LYP/6-31G(d,p) level is 6.3816 eV shown in the Table 4, which reveals that the energy gap reflects the chemical activity of the molecule. The LUMO, as an electron acceptor represents the ability to obtain an electron and HOMO represents the ability to donate an electron. The HOMO and LUMO energy gap explains the fact that eventual charge transfer interaction is taking place within the molecule. The atomic orbital compositions of the frontier molecular orbital are shown in Fig.6.

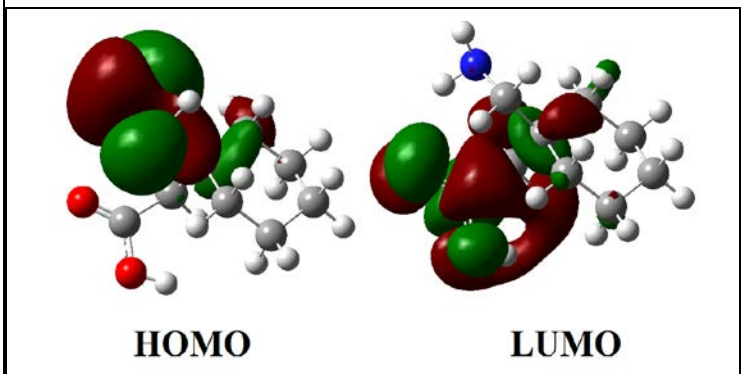

Fig. 6. Frontier molecular orbital of GBT

TABLE 4
MOLECULAR PROPERTIES OF GBT

Molecular Properties	B3LYP/6-31G(d,p)	Molecular Properties	B3LYP/6-31G(d,p)
εHOMO(eV)	-6.24560	Chemical hardness(η)	3.190829
εLUMO(eV)	- 0.136058	Chemical potential(μ)	0.313398
ε(H-L) (eV)	6.381658	Electronegativity(χ)	-3.054771
Ionization potential(I)	6.245600	Electrophilicity index(ω)	4.665812
Electron affinity(A)	-0.136058	Softness(S)	3.054771

Natural bond orbital analysis indicates that molecular orbitals are mainly composed of σ and π atomic orbital. The UV-Vis absorption spectrum of the sample GBT in the solid form is shown in Fig.7. On the basis of fully optimized ground-state structure, TD-DFT/B3LYP/6-31G(d,p) calculations have been used to determine the low-lying excited states of GBT. The calculated results involving the excitation energies and wavelength are carried out and compared experimentally with measured wavelength. It can be seen from Table 5, the calculated absorption maxima values for the title compound are 274.46 nm(gas phase) and 261.12nm(water). The measured experimental value is found at 260nm. Table 5 shows the electronic absorption wavelength(λ) and excitation energies(E) calculated by B3LYP/6-31G(d,p) along with the experimental values.

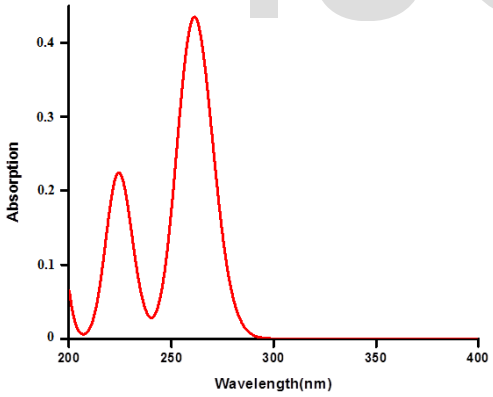

Fig. 7. UV spectra of GBT

3.3.4 Atomic charge

The charge distributions calculated by the Mulliken [25] and NBO methods for equilibrium geometry of GBT are given in Table 6. The corresponding Mulliken's plot is shown in Fig.8. The computation of the reactive atomic charges plays an important role in the application of quantum mechanical calculations for the molecular system. Mulliken atomic charges are calculated by B3LYP method with 6-31G(d,p) basis set. It is worthy to mention that C2, C5 and all hydrogen atoms exhibit positive charges, while O1, O3,C4, C6, N7, C8, C9, C10, C11 and C12 atoms exhibit negative charges. The C8 atom has a maximum negative charge value of about (-0.1648) and C2 atom has a maximum positive charge value of about (0.5803) of the title molecule GBT, calculated using B3LYP/6-31G(d,p) level of theory. Large values of charge on C8(negative) and C2(positive) are due to intramolecular charge transfer.

TABLE 5
UV-VIS EXCITATION ENERGY(ΔE) OF GBT

States	TD-B3LYP/6-31G(d,p)				Expt. λ	Major Contributions
	Gas phase		Water			
	λcal	E(eV)	λcal	E(eV)		
S1	274.46	5.5236	261.12	4.7482	260	HOMO->LUMO (89%)
S2	220.04	5.6347	224.15	5.5313	225	H-1->LUMO (72%) H-4->LUMO (6%)
S3	188.31	6.5841	191.69	6.4680	190	H-4->LUMO (13%), H-3->LUMO (27%)

TABLE 6
MULLIKEN ATOMIC CHARGES OF GBT

Atoms	B3LYP 6-31G(d,p)	Atoms	B3LYP 6-31G(d,p)	Atoms	B3LYP 6-31G(d,p)	Atoms	B3LYP 6-31G(d,p)
O1	-0.453179	C8	-0.164807	H15	0.087389	H22	0.089911
C2	0.580341	C9	-0.186988	H16	0.095984	H23	0.080604
O3	-0.477058	C10	-0.172925	H17	0.097491	H24	0.099729
C4	-0.273206	C11	-0.184469	H18	0.239823	H25	0.086630
C5	0.053955	C12	-0.196330	H19	0.261147	H26	0.105297
C6	-0.063609	H13	0.322138	H20	0.088311	H27	0.059277
N7	-0.629026	H14	0.143590	H21	0.108532	H28	0.098427
						H29	0.103019

3.3.5 Molecular transport properties

The other electronic properties much as the chemical potential (μ), electronegativity (χ), electrophilicity index (ω) and chemical hardness (η) are given in Table 4. The η, χ and μ are important tools to study the order of stability of molecular systems. Using HOMO and LUMO energies, the η and μ have been calculated. The chemical hardness and the chemical potential are given by the following expression, $\eta = (I-A)/2$, $\mu = -(I+A)/2$. The ω2, which measures the stabilization energy, has been given by the following expression, in terms of electronic chemical potential and the chemical hardness: $\omega = \mu 2/2$ electronegativity (χ), $\chi = (I+A)/2$ or $\chi = -\mu$ where I and A are ionization potential and electron affinity of a molecular system.

3.3.6 Thermodynamics properties

On the basis of vibrational analysis at B3LYP/ 6-31G(d,p) level, several thermodynamic parameters are calculated and are compared in Table 7. The zero point vibration energies

(ZPVE) and the entropy, Svib (T) calculated with B3LYP/ 6-31G(d,p) level are to the extent of accuracy and the variations in ZPVEs seem to be insignificant. The dipole moment calculated using B3LYP with 6-31G (d,p) basic set is found. The total energies and the change in the total entropy of GBT at room temperature are found to be marginal.

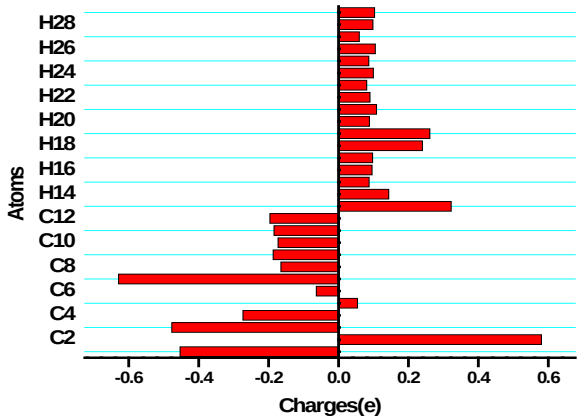

Fig. 8. Mulliken charges of GBT

TABLE 7
THERMODYNAMIC FUNCTIONS OF GBT

Parameters	B3LYP/6-31G(d,p)	Parameters	B3LYP/6-31G(d,p)
ZPVE(Kj/mol)	163.37832	**Heat capacity (CV)**	
Rotational constant x	1.29141	Total	47.645
y	0.73776	Translational	2.981
z	0.56571	Rotational	2.981
Thermal Energy (kJ/mol)	0.272396	Vibrational	41.683
Entropy (cal/mol -1K-1)		**Enthalphy(E)**	
Total	106.227	Total	170.931
Translational	41.319	Translatioanal	0.889
Rotational	30.768	Rotational	0.889
Vibrational	34.14	Vibrational	169.154
Dipole moment (Debye)			
μ_x	3.3828		
μ_y	-0.2366		
μ_z	0.6329		
Total	3.4496		

4 Conclusion

This study demonstrates that scaled DFT (B3LYP) calculations are powerful approach for understanding the vibrational spectra of the title molecule. The FT-IR, FT-Raman along with UV-spectral studies of GBT was carried out for the first time. Complete vibrational and molecular structure analyses have been performed based on the quantum mechanical approach. The differences between the observed and scaled wavenumber values of most of the fundamentals are very small. Therefore, the assignments made at DFT level of theory with only reasonable deviations from the experimental values seem to be correct. NBO analysis indicates the strong intramolecular hyperconjugative interaction within the molecule and stability of the molecule. The Mulliken charges and the natural atomic charges of the title molecule have been studied by DFT methods. The calculated HOMO and LUMO energies can be used to estimate the ionization potential, electron affinity, electronegativity, electrophilicity index, hardness, softness and chemical potential. The predicted MEP shows that the negative electrophilic potential regions are mainly localized over the oxygen atoms. The theoretically constructed FT-IR and FT-Raman show that it has a good correlation with experimentally observed FT-IR and FT-Raman spectra.

REFERENCES

[1] S.Y. Lin, S.L. Wang, "Advances in simultaneous DSC-FTIR microspectroscopy for rapid solid-state chemical stability studies: Some dipeptide drugs as examples", Advanced drug delivery reviews 2012, 64, 461-478.

[2] H. Rosner, L. Rubin, A. Kestenbaum, "Gabapentin adjunctive therapy in neuropathic pain states", The Clinical Journal of Pain 1996, 12, 56-8.

[3] C.O. Andrews, J.H. Fischer, "Gabapentin: a new agent for the management of epilepsy", Ann. Pharmacother 2005, 28, 1188-1196.

[4] J. Azizian, M. Hekmati, IHERINGIA, Sér. Bot., Porto Alegre 2014, 69, 1-8.

[5] Vânia André and M. Teresa Duarte, "Novel Challenges in Crystal Engineering: Polymorphs and New Crystal Forms of Active Pharmaceutical Ingredients", Pharmaceutical Ingredients, 69-94.

[6] H.J. Frisch, G.W. Trucks, H.B. Schlegel, G.E. Scuseria, et.al., "Official Gaussian 09 Literature Citation" Gaussian Inc., Wallingford, CT, 2003.

[7] A.D. Becke, "Density-functional thermochemistry. III. The role of exact exchange", J. Chem. Phys. 1993, 98, 5648–5652.

[8] C. Lee, W. Yang, R.G. Parr, "Development of the Colle-Salvetti correlation-energy formula into a functional of the electron density", Phys. Rev. 1988, 37, 785–789.

[9] M.J. Frisch, A.B. Nielsm, A.J. Holder, "Gaussview User Manual", Gaussian Pitsburgh, 2008.

[10] M.H. Jamróz, "Vibrational Energy Distribution Analysis VEDA 4", Warsaw, 2004.

[11] G. Ilango, M. Arivazhagan, J. Joseph Prince, V. Balechandran, "FTIR and FT-Raman spectral investigation of 2-chloro-1, 3-dibromo-5-fluorobenzene", Ind. J. Pure Appl. Phys. 2008, 46, 698.

[12] T. Gnanasambandan, S. Gunasekaran, S. Seshadri, "The Spectroscopic (FTIR, FT-Raman and UV–Vis Spectra), DFT and Normal Coordinate Computations of M-Nitromethylbenzoate", Spectrochim. Acta A 2013, 112, 52-61.

[13] K. Rastogi, M.A. Palafox, R.P. Tanwar, L. Mittal, "3,5-Difluorobenzonitrile: ab initio calculations, FTIR and Raman spectra", Spectrochim. Acta A 2002, 58, 9, 1987-2004.

[14] M. Arivazhagan, S. Jeyavijayan, J. Geethapriya, "Conformational stability, vibrational spectra, molecular structure, NBO and HOMO–LUMO analysis of 5-nitro-2-furaldehyde oxime based on DFT calcu-

lations", Spectrochim. Acta A: Mol.Biomol. Spectrosc. 2013, 104, 14–25.

[15] C. Sengamalai, M. Arivazhagan, K. Sampathkumar, "Vibrational spectral investigations of the Fourier transform infrared and Raman spectra of 2–methyl–6–nitroquinoline", Elixir Comp. Chem. 2013, 56, 13291–13298.

[16] M. Arivazhagan, R. Meenakshi, S. Prabhakaran, "Vibrational spectroscopic investigations, first hyperpolarizability, HOMO–LUMO and NMR analyzes of p-fluorobenzonitrile", Spectrochim. Acta A: Mol. Biomol. Spectrosc. 2013, 102, 59–65.

[17] G. Socrates, "Infrared and Raman Characteristic Group Frequencies – Tables and Charts", third edition, Wiley, Chichester, 2001.

[18] T. Gnanasambandan, S. Gunasekaran, S. Seshadri, "Molecular structure analysis and spectroscopic characterization of carbimazole with experimental (FT-IR, FT-Raman and UV–Vis) techniques and quantum chemical calculations", J. mol. struc, 2013, 1052, 38-49.

[19] X. Xuan, X. Wang, N. Wang, "Theoretical study of molecular structure and vibrational spectra of 1,4-dihydroxyanthraquinone", Spectrochim. Acta 2011, 79A, 1091-1110.

[20] N. Sundaraganesan, S. Ilakiamani, P. Subramani, B.D. Joshua, "Comparison of experimental and ab initio HF and DFT vibrational spectra of benzimidazole", Spectrochim. Acta 2007, 67A, 628–635.

[21] L. Jun-na, C. Zhi-rang, Y.J. Shen-Fang, "Study on the prediction of visible absorption maxima of azobenzene compounds", Zhejiang Univ. Sci. 2005, 6B, 584.

[22] P. Politzer, J.S. Murray, "Electrostatic potential analysis of dibenzo-p-dioxins and structurally similar systems in relation to theor biological activities, in: D.L. Beveridge, R. Lavery (Eds.), Theoretical Biochemistry and Molecular Biophysics: A Comprehensive Survey", Protein, vol. 2, Adenine Press, Schenectady, NY, 1991 (Chapter 13).

[23] P. Politzer, D.G. Truhler (Eds.), "Chemical Applications of Atomic and Molecular Electrostatic Potentials, Plenum Press, NY, 1981.

[24] T. Vijayakumar, I.H. Joe, V.S. Jayakumar, "Efficient π electrons delocalization in prospective push–pull non-linear optical chromophore 4-[*N*,*N*-dimethylamino]-4′-nitro stilbene (DANS): A vibrational spectroscopic study", Chem. Phys. 2008, 343, 83.

[25] R.S. Mulliken, "Electronic Population Analysis on LCAO– MO Molecular Wave Functions I", J. Chem. Phys. 1955, 23 1833–1840.